Proceedings of the Sixth International Conference on
Railway Technology: Research, Development and Maintenance
Edited by: J. Pombo
Civil-Comp Conferences, Volume 7, Paper 3.8
Civil-Comp Press, Edinburgh, United Kingdom, 2024
ISSN: 2753-3239, doi: 10.4203/ccc.7.3.8

Investigation of Critical Tunnel Length Based on the Maximum Positive Pressure on the Trailing Carriage of a High-Speed Train

Z. Sun, K. Nan, D. Guo and G. Yang

**Key Laboratory for Mechanics in Fluid Solid Coupling Systems,
Institute of Mechanics, Chinese Academy of Sciences
Beijing, China**

Abstract

The passage of a high-speed train through a tunnel exposes it to substantial tunnel pressure waves, which are heavily affected by the length of the tunnel. Although there are different criteria to determine the critical tunnel length, none of them consider the characteristics of the maximum positive pressure experienced by the trailing carriage, which has been encountered in the field tests in China. To address this problem, by dividing the process of train-tunnel interaction into three stages based on their spatial relationship, and analyzing the effects of the train wave signature, four pressure states on the train have been summarized. In particular, for the measuring points located on the trailing carriage, a maximum positive pressure can be observed when the pressure state aligns with State 4, characterized by the train wave signature reflecting at the tunnel entrance and partially passing through the measuring location. Therefore a corresponding critical tunnel length is derived based on this time relationship. Current study will shed valuable insights into the aerodynamic behavior of high-speed trains running in tunnels and contribute to the optimization of tunnel design.

Keywords: high-speed train, one-dimensional simulation method, train wave signature, critical tunnel length, train/tunnel aerodynamics, maximum positive pressure.

1 Introduction

Till the year of 2022, the number of high-speed railway tunnels in China was more than 4000, with a total length of more than 7000 km [1]. China has emerged as the

country with the highest number of high-speed railway tunnels globally. The entry of a high-speed train into a tunnel generates a compression wave ahead of the leading nose [2]. Similarly, an expansion wave forms when the trailing nose of train enters the tunnel. These waves propagate at the speed of sound and reflect upon reaching the portals of the tunnel. A complex interaction of waves arises within the tunnel due to the successive reflections of pressure waves [3]. These aerodynamic effects lead to ear discomfort of passengers and potential danger to the vehicle and tunnel facilities due to alternate pressure waves [4-5], which have drawn extensive attention and in-depth research from numerous scholars.

During the field tests on high-speed railway with 5.0m line spacing in China, it was observed that in certain short tunnels that don't adhere to the critical tunnel length formula specified in CEN 14067-5 [6]. As Fig. 1(a) shows, there is a significant increase in the maximum positive pressure on the trailing car as it passed by the tunnel. However, this phenomenon ceases as the tunnel length extends. As illustrated in Fig. 1(a), the passage of the train through the Tunnel A with a length of 274 m corresponds to the increase of maximum positive pressure on the trailing car. In contrast, when the train travels through the Tunnel B and the Tunnel C with lengths of 492m and 820m respectively, no maximum positive pressure is observed on the trailing car. Mei also encountered this phenomenon while simulating the train passing through the tunnels with different lengths [7]. The increase in maximum positive pressure on the train can potentially affect the fatigue durability of the train structure and compromise passenger comfort during the ride. Hence, this paper seeks to analyze the factors contributing to the significant increase in the maximum positive pressure on the trailing car and explore the existence of a critical tunnel length based on this phenomenon.

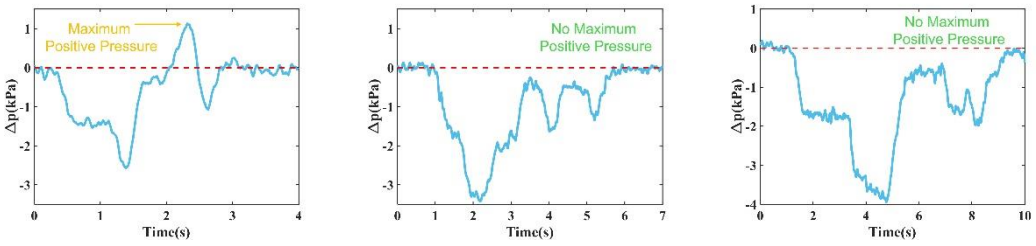

(a) (b) (c)

Figure 1. Pressure history of the point on the trailing car for different tunnel lengths: (a) Tunnel A-274m; (b) Tunnel B-492m; (c) Tunnel C-820m.

The remainder of this paper is organized as follows: Section 2 provides a description of the 1D numerical method and the validation of our code is also exhibited in this section using a full-scale train test conducted by Vardy and Reinke [8]. Taking the maximum positive pressure appearing on the trailing carriage as the determination criteria, the deriving process of the critical tunnel length is introduced in Section 3, and the validation of the formula of the critical tunnel length is also performed in this section. Finally, conclusive insights and deductions are summarized in Section 4.

2 Governing Equations

In this paper, a 1D program is developed based on a compressible and unsteady flow model. The continuity, momentum, and energy equations are represented by Eqs. (1) ~ (3).

$$\frac{\partial \rho}{\partial t} + u\frac{\partial \rho}{\partial x} + \rho\frac{\partial u}{\partial x} = 0 \tag{1}$$

$$\frac{\partial u}{\partial t} + u\frac{\partial u}{\partial x} + \frac{1}{\rho}\frac{\partial p}{\partial x} + G = 0 \tag{2}$$

$$\left(\frac{\partial p}{\partial t} + u\frac{\partial p}{\partial x}\right) - a^2\left(\frac{\partial \rho}{\partial t} + u\frac{\partial \rho}{\partial x}\right) = \left(q - \xi + uG\right)\rho\left(\kappa - 1\right) \tag{3}$$

where, u, ρ, p, and κ are the velocity, density, pressure, and specific heat ratio of air, respectively, a is the speed of sound and t is time. ξ, G, and q are the work-transfer, friction, and heat-transfer terms.

The airflow around the train inside the tunnel is treated as compressible, following the ideal gas state equation:

$$P = \rho RT \tag{4}$$

3 Critical Tunnel Length

3.1 Determination of the Maximum Positive Pressure on the Trailing Carriage

As depicted in Fig. 2, the process of a high-speed train traveling through a railway tunnel can be categorized into three stages based on the spatial relationship between the train and tunnel: train entry (Stage I), train inside the tunnel (Stage II), and train exit (Stage III). And three types of effects: a compression wave generated by the entry of the train head, friction effects during the entrance of the train body, and an expansion wave resulting from the entry of the train tail, lead to a steep pressure rise (Δp_1), a quasi-linear pressure increase (Δp_2), and a sudden pressure drop ($-\Delta p_3$), which are referred to as the train wave signature (TWS).

In these three stages, the impact of TWS on the pressure of measurement points on the train or in the tunnel exhibits distinct patterns. The lengths of the train and the tunnel are denoted as L_{TR} and L_{TU} respectively. The velocity of the train is represented by v. Furthermore, the TWS is generated with a length of L_{TR} / M [9] and propagates at the speed of sound c_0, where M refers to the Mach number, given by $M = v / c_0$

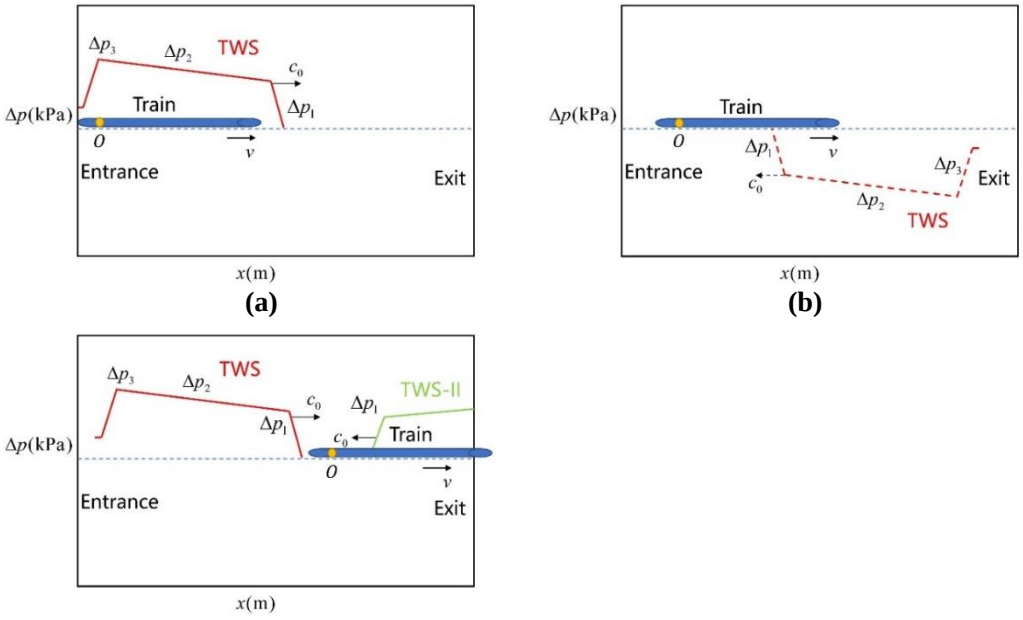

Figure 2. Spatial relationship between train and tunnel: (a) Stage I: the train enters the tunnel (b) Stage II: the train runs in the tunnel (c) Stage III: the train leaves the tunnel.

Fig. 2(a) visually portrays the spatial relationship between the train and TWS during Stage I. Point O is a measurement point along the trailing car, which remains unaffected by the compression wave originating at the entrance of the train head and propagating towards the exit, with all points on the train positioned behind it. The influence of the friction section of the TWS depends on the location of point O along the train. But the expansion wave stemming from the entrance of the train tail will invariably pass through point O, resulting in a notable pressure drop of $-\Delta p_3$. Consequently, in Stage I, the impact of TWS on point O can be represented by Eq. (5):

$$P_{\mathrm{O}}^{1} = \alpha \Delta p_2 - \Delta p_3 \tag{5}$$

Here, α is the coefficient that depends on the position of point O and takes a value between 0 and 1. When point O is near the train tail, α is equal to 0. Conversely, when point O is near the train head, α is equal to 1.

Figs. 2(b) and 2(c) present the schematic diagrams illustrating Stage II and Stage III. When the train operates within the tunnel, the TWS undergoes propagation and reflection. During a certain period of time, it is acceptable to disregard the deformation and attenuation effects of the TWS. For measurement point O, characterized by pressure p_O, the complete traversal of TWS through this point results in a modified pressure denoted as $p_O^{'}$. The relationship between p_O and $p_O^{'}$ can be expressed by Eq. (6):

$$p_O^{'} \approx p_O + \Delta p_1 + \Delta p_2 - \Delta p_3 \tag{6}$$

Here, Δp_1 , Δp_2 , and Δp_3 represent the pressure variations arising from the compression wave, the friction section, and the expansion wave, respectively.

The impact of multiple reflections of TWS on the pressure of point O is the accumulation of effects resulting from each passage of the TWS through point O. When the TWS undergoes *n* reflections, it signifies that the TWS has passed through point O *n-1* times. By applying the principle of superposition, the effects caused by the initial *n-1* passages of the TWS through point O can be expressed through a staggered series summation:

$$p_O^{21} \approx \sum_{k=1}^{n-1} (-1)^k \left(\Delta p_1 + \Delta p_2 - \Delta p_3\right) \tag{7}$$

where *n* represents the number of reflections and *n = 1* indicates the first instance of TWS reflection at the tunnel exit. The coefficient $(-1)^k$ represents the alternating nature of the TWS following each reflection.

For the *n-th* reflecting TWS, the pressure of point O is the same as the pressure situation encountered by the (*n-1*)*-th* reflecting TWS when the TWS doesn't pass to the point O. When the *n-th* reflecting TWS passes to the point O, there are two cases: partial passing and complete passing, so the influence of the *n-th* reflecting TWS can be written as a segmented function.

$$p_O^{22} = \begin{cases} (-1)^n \left(\Delta p_1 + \Delta p_2 - \Delta p_3\right), & \text{complete passing} \\ (-1)^n \left(\Delta p_1 + \beta \Delta p_2\right), & \text{partial passing} \end{cases} \tag{8}$$

The value of β is a coefficient of the position of point O, and its value is between 0 and 1.

As depicted in Eq. (9), P_{O}^1 represents the influence of TWS on the pressure at point O. It can be expressed as the summation of p_{O}^1, p_{O}^{21} and p_{O}^{22}, in accordance with the principle of superposition.

$$\begin{aligned} P_{\mathrm{O}}^1 &= p_{\mathrm{O}}^1 + p_{\mathrm{O}}^{21} + p_{\mathrm{O}}^{22} \\ &= \begin{cases} \alpha \Delta p_2 - \Delta p_3 + \sum_{k=1}^{n} (-1)^k \left(\Delta p_1 + \Delta p_2 - \Delta p_3\right) \\ \alpha \Delta p_2 - \Delta p_3 + \sum_{k=1}^{n-1} (-1)^k \left(\Delta p_1 + \Delta p_2 - \Delta p_3\right) + (-1)^n \left(\Delta p_1 + \beta \Delta p_2\right) \end{cases} \end{aligned} \tag{9}$$

Based on the predetermined definition, where $n = 1$ refers to the initial reflection of TWS at the tunnel exit, it can be deduced that TWS reflects at the exit when *n* is odd, and at the tunnel entrance when *n* is even. By considering the parity of *n*, Eq. (29) can be simplified to yield four distinct pressure states.

State 1: When *n* is odd and the *n-th* TWS completely passes point O, the pressure can be approximated as

$$P_{\mathrm{O}}^1 \approx -\Delta p_1 + (\alpha - 1) \Delta p_2 \tag{10}$$

State 2: When *n* is even and the *n-th* TWS completely passes point O, the pressure can be approximated as

$$P_{\mathrm{O}}^1 \approx \alpha \Delta p_2 - \Delta p_3 \tag{11}$$

State 3: When *n* is odd and the *n-th* TWS partially passes point O, the pressure can be approximated as

$$P_{\mathrm{O}}^{1} \approx -\Delta p_1 + (\alpha - \beta)\Delta p_2 - \Delta p_3 \tag{12}$$

State 4: When *n* is even and the *n-th* TWS partially passes point O, the pressure can be approximated as

$$P_{\mathrm{O}}^{1} \approx (\alpha + \beta - 1)\Delta p_2 \tag{13}$$

In Eqs. (10) ~ (13), Δp_1, Δp_2 and Δp_3 are approximately of the same magnitude. The values of α and β fall within the range of 0 and 1. Thus, in states 1, 2, and 3, P_{O}^{1} is consistently negative under all conditions. Only in state 4, when the sum of α and β exceeds 1, P_{O}^{1} becomes positive. This implies that during the journey of a train through the tunnel, the pressure of point O on the train is mostly negative due to the influence of TWS. This occurs because initially, the expansion wave passes through point O, resulting in negative pressure. Subsequently, the compression and expansion waves alternate passing through point O. The compression wave raises the pressure close to zero, while the expansion wave causes a rapid decrease in pressure. Only in state 4 does the pressure at point O surpass zero, which corresponds to the TWS reflecting at the tunnel exit and partially passing through point O.

As depicted in Fig. 2(c), during Stage III, when the train exits the tunnel, the TWS-II is generated. This TWS-II possesses the same intensity as the TWS-II. The TWS-II partially passes through point O, and its impact on point O is described by Eq. (14):

$$P_{\mathrm{O}}^{2} = \Delta p_1 + \gamma \Delta p_2 \tag{14}$$

where γ also represents a coefficient determined by the position of point O, and its value ranges between 0 and 1.

During Stage III, prior to the passage of the TWS-II through point O, the pressure of this point is solely influenced by the train wave TWS. As demonstrated by Eqs. (10) ~ (13), the TWS gives rise to four potential pressure states of point O. However, once the TWS-II passes through point O, the pressure at this point becomes influenced by both the TWS and the TWS-II. The influence of the TWS-II on the pressure at point O is deterministic, as defined in Eq. (14). Consequently, it is only when P_{O}^{1} is in state 4 that the superposition of P_{O}^{1} and P_{O}^{2} yields a maximum positive pressure at point O.

3.2 Derivation of the Critical Tunnel Length

As analyzed in Section 3.1, the state 4 of P_{O}^{1} corresponds to TWS partially passing through point O after reflecting at the tunnel entrance. However, more stringent conditions are required for P_{O}^{1} in State 4 to overlap with P_{O}^{2}. As depicted in Fig. 3, P_{O}^{1} is in State 4 after the compression wave passes through point O and before the expansion wave does. Only TWS-II passes through point O during this time, the superposition will occur.

The superposition condition mentioned above requires the compression wave of TWS to pass through point O when the train is leaving the tunnel, which can finally

lead to a specific relationship between the tunnel length and train length that hasn't been characterized by relevant studies.

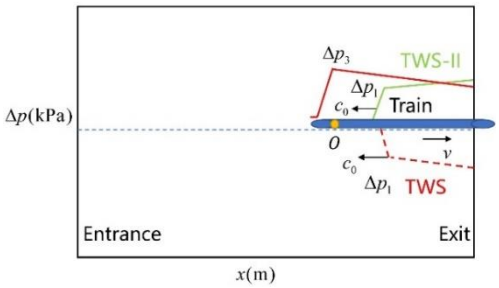

Figure 3. The relative location of TWS, TWS-II and the train.

Based on pre-defined parameters, the time T_1, at which the train head reaches the tunnel exit, is given by Eq.(15):

$$T_1 = \frac{L_{\mathrm{TU}}}{v} \tag{15}$$

Similarly, the time T_2 when the train tail reaches the tunnel exit is as Eq.(16):

$$T_2 = \frac{L_{\mathrm{TU}} + L_{\mathrm{TR}}}{v} \tag{16}$$

After the *n-th* reflection, the time it takes for the TWS to reach the tunnel portals is $(n+1)L_{\mathrm{TU}} / c_0$. It is determined that n must be an even number based on TWS reflecting at the tunnel entrance. Therefore, Assuming $n = 2m$, where m is a natural number, the time T_3 for the reflecting TWS to reach the tunnel exit is given by Eq. (17):

$$T_3 = \frac{(2m+1)L_{\mathrm{TU}}}{c_0} \tag{17}$$

According to the condition that the compression wave passes through point O as the train exits the tunnel, the relationship between T_1, T_2, and T_3 is expressed as Eq. (38):

$$T_1 < T_2 < T_3 \tag{18}$$

The relationship between the speed of sound c_0 and the speed of the train v is deduced based on the relationship between T_1 and T_3:

$$\frac{(2m+1)v}{c_0} > 1 \tag{19}$$

The relationship between the tunnel length, train length, train speed, and the number of TWS reflections is inferred based on the relationship between T_2 and T_3:

$$L_{\mathrm{TU}} < \frac{L_{\mathrm{TR}}}{\frac{(2m+1)v}{c_0} - 1} \tag{20}$$

Eq. (20) was derived based on the superposition condition of P_O^1 and P_O^2 when P_O^1 is in State 4. Therefore, when Eq. (20) is satisfied as the train passes through the tunnel, P_O^1 and P_O^2 will superimpose, resulting in a maximum positive pressure at point O. When Eq. (20) takes the limit, the tunnel length corresponds to a critical length L_{CR}:

$$L_{CR} = \frac{L_{TR}}{\frac{(2m+1)v}{c_0} - 1} \tag{21}$$

4 Conclusions and Contributions

In the current study, considering the maximum positive pressure can be expected on the trailing carriage, the critical tunnel length was derived through theoretical analysis and 1D numerical simulations. The main results are as follows:

(1) During a high-speed train passing through a tunnel, the pressure on the train experiences four states under the influence of TWS. The specific pressure state depends on the parity of the TWS reflection number and whether the TWS fully traverses the measuring position.

(2) The pressure state corresponding to State 4 occurs when the reflection number is even, and the TWS partially passes through the point on the train. In this scenario, the superposition of TWS and TWS-II results in the occurrence of maximum positive pressure for the point.

(3) Based on the relationship between the arrival time of TWS at the tunnel exit and the time of the leading and trailing nose of the train reaching the tunnel exit, a critical tunnel length associated with the maximum positive pressure on the trailing carriage is derived. When the tunnel length is shorter than the critical tunnel length, a maximum positive pressure is observed in the pressure history of the point on the trailing car.

Acknowledgements

This research was funded by the China National Railway Group Science and Technology Program grant (K2023J047) and the Research Major Project of China Academy of Railway Sciences Group Co., Ltd (2023YJ277).

References

[1] Gong, J., Wang, W., li, X., 2023. Statistics of railway tunnels in China by the end of 2022 and overview of key tunnels of projects newly put into operation in 2022. Tunnel Construction 4, 721–738.

[2] Okubo, H., Miyachi, T., Sugiyama, K., 2021. Pressure fluctuation and a micro-pressure wave in a high-speed railway tunnel with large branch shaft. Journal of Wind Engineering and Industrial Aerodynamics 217, 104751.

[3] Raghunathan, R. S., Kim, H.-D., & Setoguchi, T. (2002). Aerodynamics of high-speed railway train. *Progress in Aerospace Sciences*, *38*(6–7), 469–514. https://doi.org/10.1016/S0376-0421(02)00029-5

[4] Niu, J., Zhou, D., Liu, F., Yuan, Y., 2018. Effect of train length on fluctuating aerodynamic pressure wave in tunnels and method for determining the amplitude of pressure wave on trains. Tunnelling and Underground Space Technology 80, 277–289.

[5] Tabarra, M., Sturt, R. & Arup, U. (2010). High Speed Rail Tunnel Aerodynamics: Transient pressure and loadings on fixed tunnel equipment. *Proceedings of the 7th UIC World Congress on High Speed Rail*, Beijing, China, pp. 7–9.

[6] CEN European Standard. (2010). Railway Applications—Aerodynamics—Part 5: Requirements and Test Procedures for Aerodynamics in Tunnels. CEN EN 14067-5.

[7] Mei, Y., Zhang, Z., Du, J., 2021. Numerical Simulation of External Pressure Caused by High-Speed Maglev Single Train Passing Tunnel. CHINA RAILWAY SCIENCE 42, 78–89.

[8] Vardy, A. E., & Reinke, P. (1999). Estimation of train resistance coefficients in tunnels from measurements during routine operation. *Proceedings of the Institution of Mechanical Engineers, Part F: Journal of Rail and Rapid Transit*, *213*(2), 71–87. https://doi.org/10.1243/0954409991531047

[9] William-Louis, M. J. P., & Tournier, C. (1998). Non-homentropic flow generated by trains in tunnels with side branches. *International Journal of Numerical Methods for Heat & Fluid Flow*, *8*(2), 183–198. https://doi.org/10.1108/09615539810201730